Stress Triggering of the 1999 Hector Mine Earthquake by Transient Deformation Following the 1992 Landers Earthquake

Fred F. Pollitz

U.S. Geological Survey
345 Middlefield Road, MS 977
Menlo Park, CA 94025

I. Selwyn Sacks

Carnegie Institution of Washington
Department of Terrestrial Magnetism
5241 Broad Branch Road, N.W.
Washington, DC 20015

Submitted to

Bulletin of the Seismological Society of America

November, 2000

Abstract

The M=7.3 June 28, 1992 Landers and M=7.1 October 16, 1999 Hector Mine earthquakes, California, both right lateral strike-slip events on NNW-trending subvertical faults, occurred in close proximity in space and time in a region where earthquake recurrence times are thousands of years. This suggests a causal role for the Landers earthquake in triggering the Hector Mine earthquake. Previous modeling of the static stress change associated with the Landers earthquake shows that the area of peak Hector Mine slip lies where the Coulomb failure stress promoting right-lateral strike-slip failure was high, but the nucleation point of the Hector rupture was neutrally to weakly promoted, depending on the assumed coefficient of friction. Possible explanations that could account for the 7-year delay between the two ruptures include background tectonic stressing, dissipation of fluid pressure gradients, rate and state-dependent friction effects, and post-Landers viscoelastic relaxation of the lower crust and upper mantle. By employing a viscoelastic model calibrated by geodetic data collected during the time period between the Landers and Hector Mine events, we calculate that postseismic relaxation produced a transient increase in Coulomb failure stress of about 0.7 bars on the impending Hector Mine rupture surface. The increase is greatest over the broad surface that includes the 1999 nucleation point and the site of peak slip further north. Since stress changes of magnitude $\geq$ 0.1 bar are associated with documented causal fault interactions elsewhere, viscoelastic relaxation likely contributed to the triggering of the Hector Mine earthquake. This interpretation relies on the assumption that the faults occupying the central Mojave Desert (i.e., both the Landers and Hector Mine rupturing faults) were critically stressed just prior to the Landers earthquake.

Introduction

Paired earthquakes -- the occurrence of one large earthquake close in space and time to a preceding one -- are known on timescales of seconds (e.g., 1998 Antarctic Plate earthquake (Henry et al., 2000)), hours (e.g., Landers-Big Bear sequence (Wald and Heaton, 1994; King et al., 1994)), months (August, 1999 Izmit - November, 1999 Düzce, Turkey earthquakes), years (1944 Tonankai - 1946 Nankaido earthquakes (Ando, 1975)), and possibly decades (Pollitz et al., 1998). The M=7.1 October 16, 1999 Hector Mine, California, earthquake was a right-lateral strike-slip event in the central Mojave Desert (Figure 1). It occurred 7 years after the M=7.3 June 28, 1992 Landers earthquake along a parallel fault section about 30 km northeast of the Landers source region. Both earthquakes occurred within a part of the active Eastern California Shear Zone where earthquake recurrence times are estimated to be about 4000 years (Sauber et al., 1994; Rubin and Sieh, 1997).

The problem of explaining the time delay between paired earthquakes or mainshock/aftershock sequences hasstimulated several proposed mechanisms (see review by Harris, 1998), including pore fluid flow (Jaume and Sykes, 1992), rate and state-dependent friction (Dieterich, 1994;Gomberg et al., 1998), and postseismic viscoelastic flow in the lower crust (Deng et al., 1999). The first two mechanisms act to weaken the secondary fault with time, while the third changes the stress resolved on it, in some cases compounding the static stress change. Typical mainshock-aftershock sequences in the upper continental crust occur on timescales of days to years. The rate and state-dependent friction model has successfully explained the decay rate of aftershock sequences (Dieterich, 1994; Gross and Kisslinger, 1997; Gross and Bürgmann, 1998), and it relies on the combination of static stress change from the mainshock and background loading rate to trigger a population of secondary faults. The rate of occurrence of Landers aftershocks in the epicentral region had effectively returned to pre-Landers seismicityrates about 3 years after the Landers earthquake (Gross and

Kisslinger, 1997). The spatial pattern of aftershock activity is generally well explained in terms of a change in static Coulomb failure stress (King et al., 1994; Stein, 1999). The Landers - Hector earthquake pair is atypical because of the relatively long delay, because the background loading rate is small, and because the nucleation point of the Hector rupture lies in a neutral to weakly encouraged zone of static stress change from the Landers earthquake, depending on the coefficient of friction (Plate 2c of Parsons and Dreger, 2000).

Here we investigate whether postseismic relaxation of the lower crust and mantle following the Landers earthquake could have contributed significant postseismic stress to the future Hector rupture area. This is motivated by the observation of elevated horizontal strain rates in the central Mojave Desert for several years following the Landers earthquake (Savage and Svarc, 1997), complemented by large transient vertical motions (Peltzer et al., 1998). These anomalously high rates appear best explained by deep viscoelastic relaxation (Deng et al., 1998; Pollitz et al., 2000). While the model of Deng et al. (1998) consists of a weak lower crust and strong upper mantle beneath the Mojave Desert, the model of Pollitz et al. (2000) consists of a stronger lower crust underlain by a weak mantle. We prefer this model because it was derived on the basis of much more data than was available to Deng et el. (1998). A sharp increase in strength with depth at the crust-mantle transition has long been assumed for continental regions on the basis of the relative strength of lower crustal materials (i.e., granulite) and olivine, but the strength contrast also depends on the local temperature gradient and water content of olivine, factors which may be especially important in tectonically active regions. In fact, a relatively ductile upper mantle has been inferred in all studies of tectonically active regions where data resolution allows sufficient sensitivity to mantle flow. This includes postseismic relaxation investigations made around subduction zones (e.g., Thatcher et al., 1980; Miyashita, 1987; Rydelek and Sacks, 1990), around the NE Rift Zone, Iceland (Hofton and Foulger,

1996; Pollitz and Sacks, 1996), and in the Mojave Desert (Pollitz et al., 2000), post-lake-drainage studies in the Basin and Range Province (e.g., Bills et al., 1994), and post-glacial rebound studies of Iceland (Sigmundsson and Einarsson, 1992) and the Pacific northwest (James et al., 2000).

The choice of viscoelastic stratification affects the magnitude and distribution of regional postseismic stress. In the present study we employ the weak-upper mantle viscoelastic model of Pollitz et al. (2000) in order to estimate post-Landers stress changes. We find that the Coulomb failure stress in the Hector rupture area increased by several tenths of a bar during the period 1992 to 1999, was positive over nearly the entire Hector rupture area, and (where positive) exceeded the Landers static stress change over about 50% of the Hector rupture area.

Postseismic Stress Model

The viscoelastic stratification used in this study is shown in Figure 2 and consists of an elastic upper crust underlain by ductile lower crust and upper mantle. It was derived from a grid search for a set of viscosities in a one-layer lower crust and two-layer upper mantle which, in conjunction with the known elastic stratification, best explains postseismic geodetic measurements made after the Landers earthquake (Pollitz et al., 2000). A robust feature of the geodetic modeling is that the mantle is highly ductile, and bulk relaxation of the mantle has shaped the post-Landers crustal deformation field more strongly than lower crustal relaxation. The fit of this model to the surface horizontal velocity field over the period 1992-1995 (post-Landers and pre-Hector) is shown in Figure 3. We assume that the viscoelastic model is well calibrated by these data and is suitable for calculating time-dependent stress evolution at all upper crustal depths and all times following the Landers earthquake. As in Pollitz et al. (2000), we calculate time-dependent postseismic strain in a gravitational elastic-viscoelastic coupled medium using the method of Pollitz (1997). Static strain changes

in a depth-dependent elastic model are calculated using the method of Pollitz (1996). From these strains the stresses are calculated using the depth distribution of isotropic elastic constants of Figure 2.

To calculate both static and postseismic stress changes we use the distributed slip model of Wald and Heaton (1994) for the Landers earthquake and the Jones and Helmberger (1993) model for the M=6.5 June 28 1992 Big Bear earthquake, which occurred just 3 hours after and 30 km SW of the Landers earthquake. The static stress pattern around the Landers rupture is sensitive to the choice of Landers coseismic model (Parsons and Dreger, 2000; R. Harris, manuscript submitted to this volume), but the postseismic stress change is found to depend little on this choice. For this reason as well as consistency with the Parsons and Dreger study, we use the Wald and Heaton (1994) model for the coseismic rupture. The Big Bear stress changes are found to have only a small effect on the stress evolution in the Hector Mine rupture area.

Stress Evolution

We evaluate the change in Coulomb failure stress defined by

$$\Delta\sigma_f = \Delta\tau + \mu' \Delta\sigma_n \quad (1)$$

where $\Delta\tau$ is the change in shear stress (positive for right-lateral shear), $\Delta\sigma_n$ is the change in normal stress (positive tensile), and μ' is the effective coefficient of friction. Both $\Delta\tau$ and $\Delta\sigma_n$ are evaluated on a secondary fault surface with specified orientation. The best-fitting point source for the Hector Mine earthquake is right-lateral strike-slip faulting on a N29˚W-striking plane dipping 77˚ NE (U.S. Geological Survey, Southern California Earthquake Center, and California Division of Mines and Geology, 2000, hereafter U.S.G.S. et al., 2000). The earthquake, however, ruptured two principal faults (Figure 1): the southern portion of the Bullion fault, which strikes NW, and the Lavic Lake fault further north, which strikes NNW near its junction with the Bullion fault but curves to a more westerly trend further north. We represent the potentially

failing Hector rupture surface as a single N29˚W striking, 48 km long vertical fault for two reasons: 1. This is the average strike of the Lavic Lake segment where rupture nucleated and where most of the slip was concentrated (U.S.G.S. et al., 2000), and 2. Postseismic stress changes in this locality are insensitive to small to moderate changes in the strike and dip of the secondary fault plane. The chosen fault plane spans the area of significant surface rupture (U.S.G.S. et al., 2000).

We consider two values of the effective coefficient of friction, $\mu' = 0.3$ and $\mu' = 0.7$. The first value is typical of that inferred for faults with tens of km of cumulative slip (Stein, 1999), while the second value is that expected from rock mechanics experiments (Lachenbruch and McGarr, 1990), and appears typical for immature faults (Stein, 1999). The best correlation of Landers aftershocks with the static Coulomb failure stress change has been obtained with $\mu' = 0.85$ (Seeber and Armbruster, 2000). This suggests that a relatively large value of μ' is appropriate for the Hector Mine rupture area. Figure 4 shows the regional pattern of $\Delta\sigma_f$ with $\mu' = 0.7$ just after the Landers/Big Bear earthquakes and just before the Hector Mine earthquake at depth 7 km, approximately the depth of the Hector Mine nucleation point. Just after the Landers earthquake (Figure 4a), the southern 60% of the future Hector rupture was located in a stress shadow (negative $\Delta\sigma_f$), and the northern 40% lay in a stress-encouraged zone, $\Delta\sigma_f$ reaching up to 2.9 bars. The nucleation point was neither encouraged or discouraged. This picture is altered by the addition of 7.3 years of post-Landers crust and mantle relaxation (Figure 4b), with the magnitude and spatial extent of the stress-encouraged zone increasing by > 0.5 bars over the northern 50% of the Hector Mine rupture zone. This is seen more clearly in the depth sections of $\Delta\sigma_f$ shown in Figure 5. In the intervening 7.3 years, the nucleation point passed from being encouraged at $\Delta\sigma_f = 0.0$ bars to being encouraged at $\Delta\sigma_f \sim 0.7$ bars, a value which is known to produce strong correlations with triggered seismicity in static Coulomb failure stress studies (Stein, 1999). The stress encouragement was amplified on the

entire portion of the Hector rupture for which the static stress change was positive, the postseismic stress change exceeded the static stress change over approximately the middle 50% of the Hector rupture, and the maximum $\Delta\sigma_f$ on the Hector rupture plane increased from 2.9 to 3.7 bars.

These calculations are very sensitive to the choice of μ'. Figure 6 shows the depth profiles of $\Delta\sigma_f$ obtained with $\mu' = 0.3$. The zone of stress encouragement from the Landers static stress change is reduced in both magnitude and spatial extent with the smaller coefficient of friction. This is because the static shear stress change $\Delta\tau$ is negative over almost the entirety of the Hector Mine rupture zone while the static normal stress change is positive (i.e., tensile) over the northern half, and the Coulomb stress change in (1) is strongly dependent on the coefficient of friction, also found by Parsons and Dreger (2000). In this case the Hector Mine nucleation point evolves from an initial -0.7 bars stress shadow (Figure 6a) to -0.1 bars at the time of the Hector Mine earthquake (Figure 6b). The viscoelastic relaxation contribution is only weakly sensitive to μ' (compare Figures 5c and 6c) because most of the postseismic $\Delta\sigma_f$ results from the shear stress change $\Delta\tau$. In this case, the postseismic stress change exceeds the coseismic stress change over about 75% of the Hector rupture. Regardless of the value of the coefficient of friction, the calculations of the stress evolution model point strongly towards viscoelastic relaxation of the lower crust and mantle following the Landers earthquake as contributing to the triggering of the Hector Mine earthquake.

Discussion

The Hector Mine earthquake may be considered as the fourth event in a cascade of recent large Mojave Desert earthquakes, preceded by the 1992 Joshua Tree, 1992 Landers, and 1992 Big Bear earthquakes. Each event, beginning with the Joshua Tree earthquake, stressed the rupture zone of the succeeding event by ~1 bar (King et al.,

1994). The inclusion of the Hector Mine earthquake in this succession is based on the fact that, according to our model with $\mu' = 0.7$, the viscoelastic stress change rate over much of the Hector rupture zone averaged 0.1 bars/yr during the time period between the Landers and Hector Mine earthquakes. This is about 3 times greater than the interseismic stress accumulation rate based on pre-Landers geodetic measurements of strain accumulation in the Mojave Desert (Sauber et al., 1994; Savage and Svarc, 1997, p. 7575; Shen et al., 1996) and is comparable with the stress accumulation rate on the San Andreas fault based on geodetic measurements (e.g., Savage et al., 1986). Nevertheless, the accumulated 0.7 bars is much less than the ~20 bars stress drop expected for a strike-slip earthquake of this magnitude (Kanamori and Anderson, 1975). Analysis of fault state based on friction mechanics indicate that a small positive stress step will lead to short term triggering of earthquakes only if the secondary fault being considered is already near failure (Figure 3 of Gomberg et al., 1998). This conclusion agrees with a cellular automota model study of the response to a small stress perturbation by a fault system characterized by a highly heterogeneous absolute stress distribution (Rydelek and Sacks, 1999). This suggests that the Hector rupture zone was already critically stressed just prior to the Landers earthquake.

The accumulated viscoelastic stress change is remarkably well correlated with the Hector Mine coseismic slip distribution (Figures 5 and 6). This may be coincidental, or it may reflect a stress concentration capability which is unique to a slow transient (versus sudden static) stress change. The effectiveness of viscoelastic relaxation of the sub-lithosphere for triggering earthquakes was demonstrated by a statistical correlation between land (intraplate) and trench (interplate) earthquakes in northern Honshu, Japan (Rydelek and Sacks, 1988, 1990). Transient postseismic $\Delta\sigma_f$ of 1 to 3 bars accumulated over decades have been correlated with the occurrence of the 1995 Kobe earthquake (Pollitz and Sacks, 1997), the 1944 Tonankai earthquake (Pollitz and Sacks, 1995), and the inhibition of the anticipated "Tokai" earthquake in Suruga Bay, Japan

(Pollitz and Sacks, 1995). Transient postseismic stress is also believed to play a role in the generation of repeated earthquakes in the New Madrid Seismic Zone (Kenner and Segall, 2000). At a much shorter timescale, transient stress changes have been correlated with the occurrence of post-Northridge aftershocks (Deng et al., 1999). If the transient stresses generated by viscoelastic relaxation of the lower crust and mantle are capable of bringing major faults closer to (or away from) failure, as suggested by these studies, then its potential impact should be closely examined in regions surrounding major historic earthquake ruptures.

Acknowledgements. This work was partially supported by the IGPP Program of Lawrence Livermore National Laboratory while Pollitz was a postdoctoral researcher at UC Davis. We thank Doug Dreger for providing the slip distribution of the Hector Mine earthquake depicted in Figures 5 and 6. This paper has benefited from constructive criticisms by Ross Stein and Tom Parsons.

References

Ando, M., 1975. Source mechanisms and tectonic significance of historical earthquakes along the Nankai Trough, Japan, *Tectonophysics, 27*, 119-140.

Bills, B.G., D.R. Currey, and G.A. Marshall, 1994. Viscosity estimates for the crust and upper mantle from patterns of lacustrine shoreline deformation in the Eastern Great Basin, *J. Geophys. Res., 99*, 22059-22086.

Deng, J., M. Gurnis, H. Kanamori, and E. Hauksson, 1998. Viscoelastic flow in the lower crust after the 1992 Landers, California, earthquake, *Science, 282*, 1689-1692.

Deng, J.S., K. Hudnut, M. Gurnis, and E. Hauksson, 1999. Stress loading from viscous flow in the lower crust and triggering of aftershocks following the 1994 Northridge California, earthquake, *Geophys. Res. Lett., 26*, 3209-3212.

Dieterich, J.H., 1994. A constitutive law for rate of earthquake production and its application to earthquake clustering, *J. Geophys. Res., 99*, 2601-2618.

Gomberg, J., N.M. Beeler, M.L. Blanpied, and P. Bodin, 1998. Earthquake triggering by transient and static deformations, *J. Geophys. Res., 103*, 24,411-24,426.

Gross, S. and C. Kisslinger, 1997. Estimating tectonic stress rate and state with Landers aftershocks, *J. Geophys. Res., 102*, 7603-7612.

Gross, S.J. and R. Bu¨rgmann, 1998. Rate and state of background stress estimated from the aftershocks of the 1989 Loma Prieta earthquake, *J. Geophys. Res., 103*, 4915-4927.

Harris, R.A., 1998. Introduction to special section: Stress triggers, stress shadows, and implications for seismic hazard, *J. Geophys. Res., 103*, 24,347-24,358.

Hector Mine Earthquake Geologic Working Group, 2000. Preliminary surface rupture and slip distribution associated with the M7.1 Hector Mine earthquake of 16 October 1999, *Bull. Seismol. Soc. Am., submitted* (this issue).

Henry, C., S. Das, and J.H. Woodhouse, 2000. The great March 25, 1998 Antarctic Plate earthquake: Moment tensor and rupture history, *J. Geophys. Res., 105*, 16,097-16,118.

Hofton, M.A. and G.R. Foulger, 1996. Postrifting anelastic deformation around the spreading plate boundary, North Iceland, 1, Modeling of the 1987-1992 deformation field using a viscoelastic Earth structure, *J. Geophys. Res., 101*, 25,403-25,421.

James, T.S., J.J. Clague, K. Wang, and I. Hutchinson, 2000. Postglacial rebound at the northern Cascadia subductionn zone, *Quater. Sci. Rev., 19*, 1527-1541.

Jaume, S.C and L.R. Sykes, 1992. Changes in state of stress on the southern San Andreas fault resulting from the California earthquake sequence of April to June 1992, *ence, 258*, 1325-1328.

Jones, L.E. and D.V. Helmberger, 1993. Source parameters of the 1992 Big Bear

sequence, *Eos Trans. AGU, 74*(16), Spring Meet. Suppl., 215.

Kanamori, H. and D.L. Anderson, 1975. Theoretical basis of some empirical relations in seismology, *Bull. Seis. Soc. Am., 65*, 1073-1095.

King, G.C., R.S. Stein, and J. Lin, 1994. Static stress changes and the triggering of earthquakes, *Bull. Seism. Soc. Am., 84*, 935-953.

Lachenbruch, A.H. and A. McGarr, 1990. Stress and heat flow on the San Andreas fault, *U.S. Geol. Surv. Prof. Pap. 1515*, 261-277.

Miyashita, K., 1987. A model of plate convergence in southwest Japan, inferred from leveling data associated with the 1946 Nankaido earthquake, *J. Phys. Earth, 35*, 449-467.

Peltzer, G., P. Rosen, F. Rogez, and K. Hudnut, 1998. Poro-elastic rebound along the Landers 1992 earthquake surface rupture, *J. Geophys. Res., 103*, 30,131-30,145.

Pollitz, F.F., 1996. Coseismic deformation from earthquake faulting on a layered spherical Earth, *Geophys. J. Int., 125*, 1-14.

Pollitz, F.F., 1997. Gravitational-viscoelastic postseismic relaxation on a layered spherical Earth, *J. Geophys., Res., 102*, 17,921-17,941.

Pollitz, F.F., R. Bürgmann, and B. Romanowicz, 1998. Viscosity of oceanic asthenosphere inferred from remote triggering of earthquakes, *Science, 280*, 1245-1249.

Pollitz, F.F., G. Peltzer, and R. Bürgmann, 2000. Mobility of continental mantle: Evidence from postseismic geodetic observations following the 1992 Landers earthquake, *J. Geophys. Res., 105*, 8035-8054.

Pollitz, F.F. and I.S. Sacks, 1995. Consequences of stress changes following the 1891 Nobi earthquake, Japan, *Bull. Seis. Soc. Am., 85*, 796-807.

Pollitz, F.F. and I.S. Sacks, 1996. Viscosity structure beneath northeast Iceland, *J. Geophys. Res., 101*, 17,771-17,793.

Pollitz, F.F. and I.S. Sacks, The 1995 Kobe, Japan, earthquake: A long-delayed aftershock of the offshore 1944 Tonankai and 1946 Nankaido earthquakes, *Bull.*

Seis. Soc. Am, 87, 1-10, 1997.

Rubin, C.M. and K. Sieh, 1997. Long dormancy, low slip rate, and similar slip-per-event for the Emerson fault, eastern California shear zone, *J. Geophys. Res., 102*, 15,319-15,333.

Rydelek, P.A. and I.S. Sacks, 1988. Asthenospheric viscosity inferred from correlated land–sea earthquakes in north–east Japan, *Geophys. J. Int., 336*, 234-237.

Rydelek, P.A. and I.S. Sacks, 1990. Asthenospheric viscosity and stress diffusion: a mechanism to explain correlated earthquakes and surface deformations in northeast Japan, *Geophys. J. Inter., 100*, 39-58.

Rydelek, P.A. and I.S. Sacks, 1999. Large earthquake occurrence affected by small stress changes, *Bull. Seismol. Soc. Am., 89*, 822-828.

Sauber, J., W. Thatcher, S.C. Solomon, and M. Lisowski, 1994. Geodetic slip rate for the Eastern California Shear Zone and the recurrence time of Mojave Desert earthquakes, *Nature, 367*, 264-266.

Savage, J.C., W.H. Prescott, and G. Gu, 1986. Strain accumulation in southern California, *J. Geophys. Res., 91*, 7455-7473.

Savage, J.C., and J.L. Svarc, 1997. Postseismic deformation associated with the 1992 M_w = 7.3 Landers earthquake, southern California, *J. Geophys. Res., 102*, 7565-7577.

Seeber, L. and J.G. Armbruster, 2000. Earthquakes as beacons of stress change, *Nature, 407*, 69-72.

Shen, Z.-K., D.D. Jackson, and B.X. Ge, 1996. Crustal deformation across and beyond the Los Angeles basin from geodetic measurements, *J. Geophys. Res., 101*, 27,957-27,980.

Sieh, K., et al., 1993. Near-field investigations of the Landers earthquake sequence, April to July 1992, *Science, 260*, 171-176.

Sigmundsson, F. and P. Einarsson, 1992. Glacio-isostatic crustal movements caused

by historical volume change of the Vatnajokull ice cap, Iceland, *Geophys. Res. Lett., 19*, 2123-2126.

Stein, R.S., 1999. The role of stress transfer in earthquake occurrence, *Nature, 402*, 605-609.

Thatcher, W., T. Matsuda, T. Kato, and J.B. Rundle, 1980. Lithospheric loading by the 1896 Riku–u earthquake, northern Japan: Implications for plate flexure and asthenospheric rheology, *J. Geophys. Res., 85*, 6429-6435.

U.S. Geological Survey, Southern California Earthquake Center, and California Division of Mines and Geology, 2000. Preliminary Report on the 16 October M 7.1 Hector Mine, California Earthquake, *Seismol. Res. Lett., 71*, 11-23.

FIGURE CAPTIONS

Figure 1. Active faults in the western-central Mojave Desert and epicenters of $M \geq 5$ earthquakes from April, 1992 to August, 2000. The surface ruptures of the 1992 Landers and 1999 Hector Mine earthquakes (Sieh et al., 1993; Hector Mine Earthquake Geologic Working Group, 2000) are shown as heavy red and orange lines, respectively.

Figure 2. Viscoelastic stratification of the central Mojave Desert based on the geodetic modeling of Pollitz et al. (2000). Viscosity values are indicated in the one-layer lower crust and two-layer mantle. For simplicity, a homogeneous mantle is assumed from depth 50 km to the base of the model at depth 1000 km.

Figure 3. Observed horizontal velocity with respect to a fixed site from November, 1992 to December, 1995 and corresponding 1 σ error ellipses obtained from Global Positioning System measurements by the U.S. Geological Survey (U.S.G.S.) and Southern California Earthquake Center (SCEC). Superimposed as black arrow are horizontal velocity vectors resulting from lower crust and mantle relaxation following the Landers and Big Bear earthquakes, calculated using appropriate Landers and Big Bear coseismic rupture models (see text) and the viscoelastic stratification of Figure 2 (after Pollitz et al., 2000).

Figure 4. Snapshots of change in Coulomb failure stress $\Delta\sigma_f$ at depth 7 km (a) just after the 1992 Landers earthquake and (b) just before the 1999 Hector Mine earthquake, assuming an effective coefficient of friction of 0.7. The difference between the two images arises from the postseismic stress change from viscoelastic relaxation of the lower crust and mantle accumulated during the 7.3 years between the two earthquakes. Representative fault surfaces for the Landers, Big Bear, and Hector Mine earthquakes are indicated by white lines, and the Hector

Mine nucleation point by a red "*". Epicenters of earthquakes with magnitude ≥ 3.0 and depth 2-12 km are superimposed, covering the time periods (a) 07/01/92-12/31/92 and (b) 10/15/97-10/15/99.

Figure 5. Depth profile of change in Coulomb failure stress $\Delta\sigma_f$ derived from (a) the Landers static stress change, (b) the static stress change plus the total postseismic stress change at the time of the Hector Mine earthquake, and (c) the postseismic stress change alone. The stress changes are calculated on potentially failing vertical faults striking N29˚W and passing through the Hector Mine nucleation point (indicated by a black star), with effective coefficient of friction $\mu' = 0.7$. Superimposed in (c) is the projection of the right-lateral slip distribution of the Hector Mine earthquake (Parsons and Dreger, 2000)

Figure 6. Depth profile of change in Coulomb failure stress $\Delta\sigma_f$ as in Figure 5, with $\mu' = 0.3$.

Figure 1

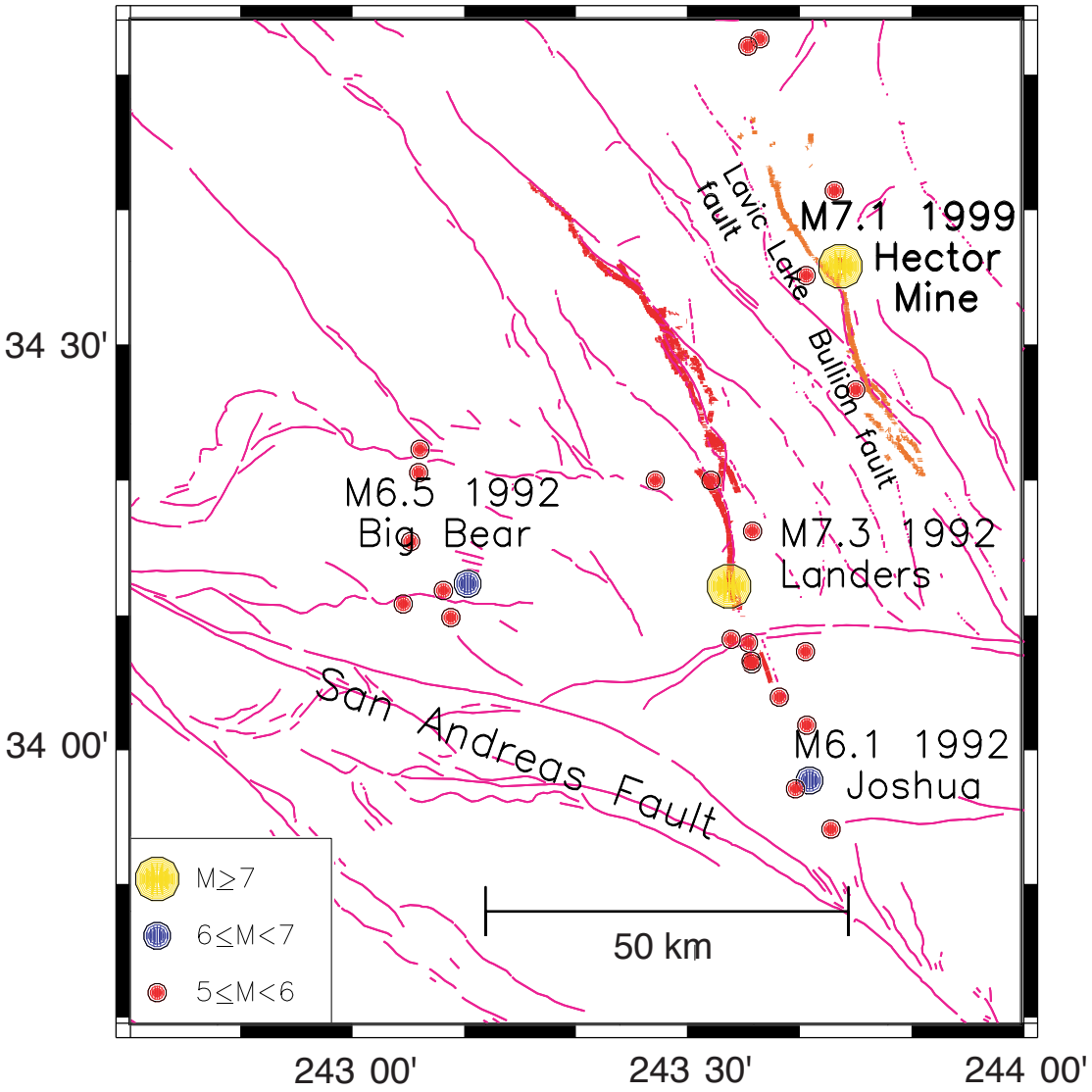
M7.1 1999
Hector
Mine
Lavic Lake
fault
Bullion fault
M6.5 1992
Big Bear
M7.3 1992
Landers
San Andreas Fault
M6.1 1992
Joshua
M≥7
6≤M<7
5≤M<6
50 km
34 30'
34 00'
243 00'
243 30'
244 00'

Figure 2

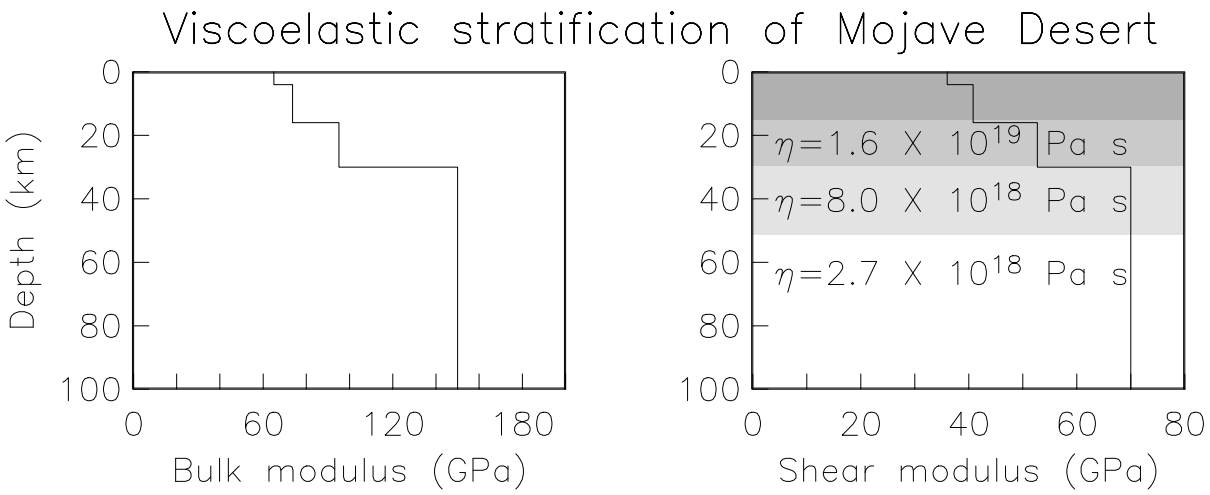

Figure 3

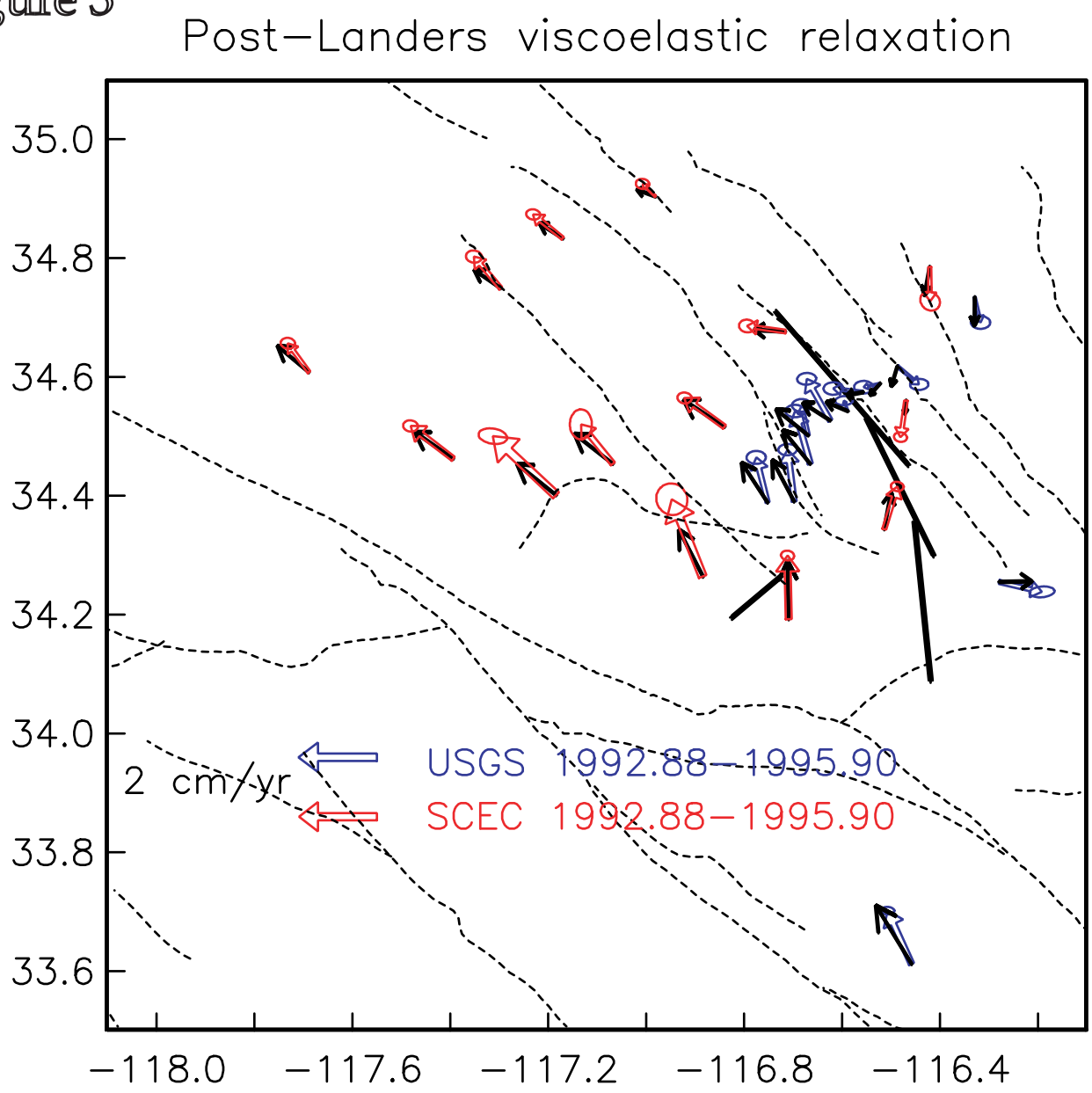

Figure 4

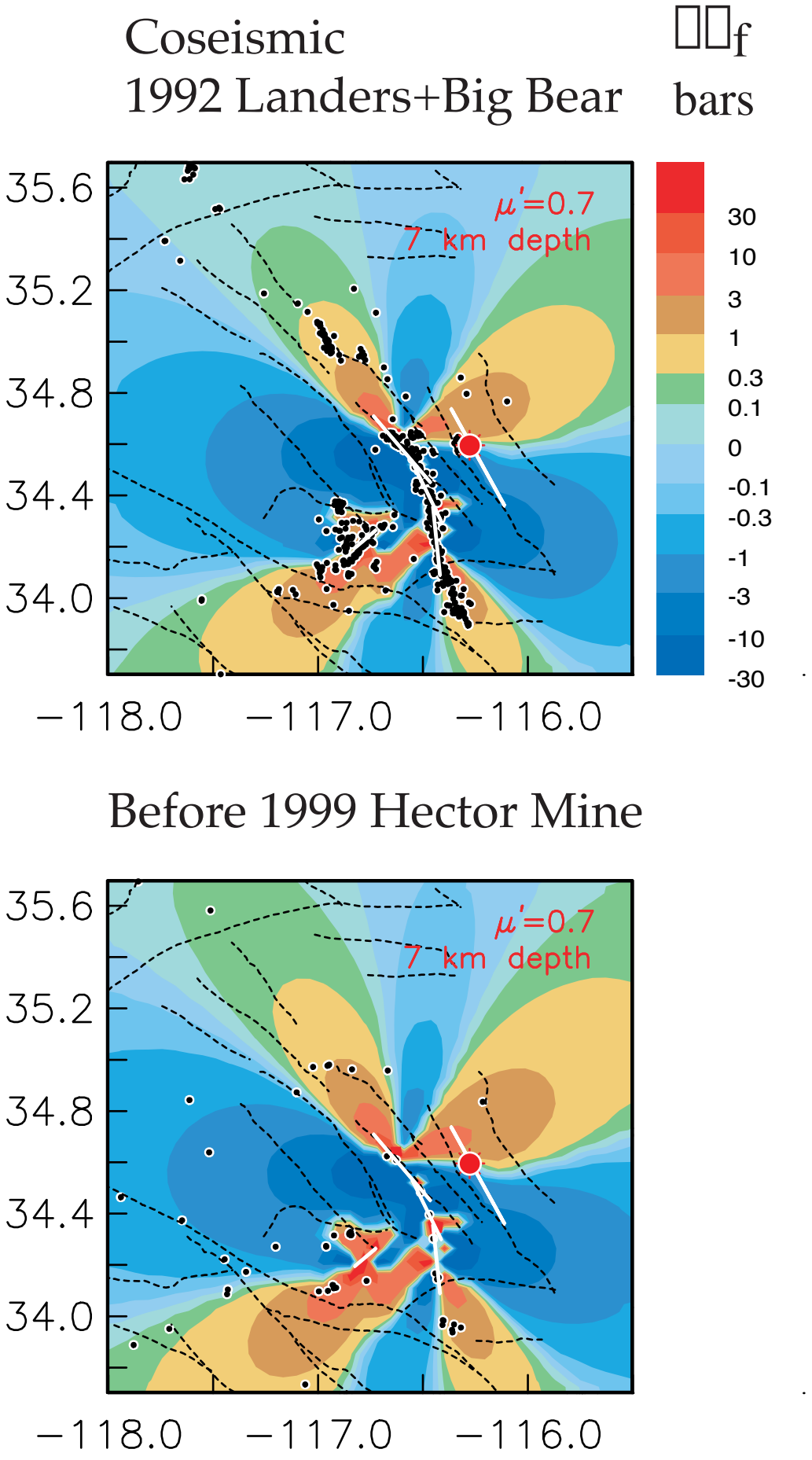
Coseismic
1992 Landers+Big Bear
□□f
bars
μ'=0.7
7 km depth
30
10
3
1
0.3
0.1
0
-0.1
-0.3
-1
-3
-10
-30
35.6
35.2
34.8
34.4
34.0
−118.0
−117.0
−116.0
Before 1999 Hector Mine
μ'=0.7
7 km depth
35.6
35.2
34.8
34.4
34.0
−118.0
−117.0
−116.0

Figure 5

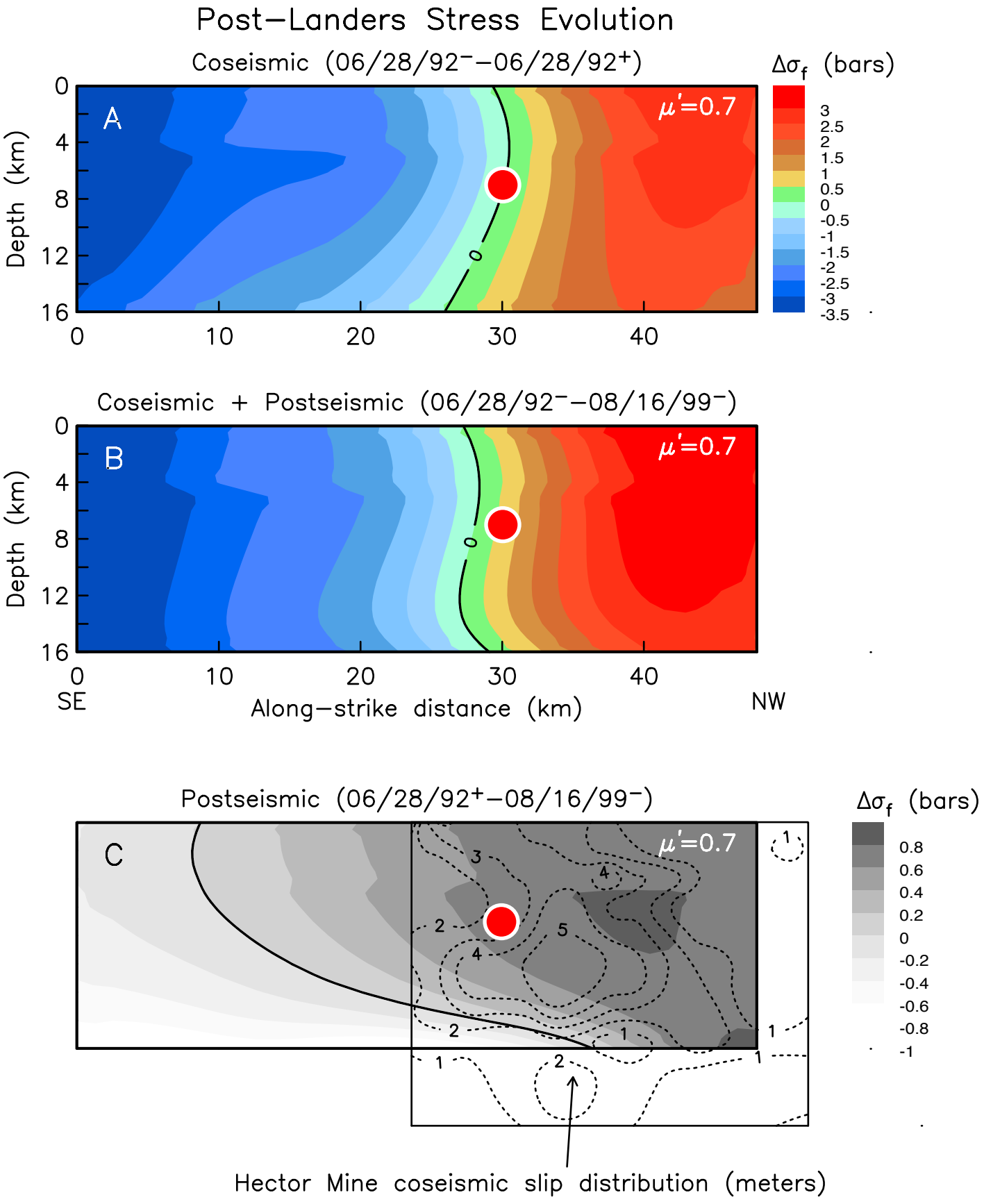
Post–Landers Stress Evolution
Coseismic (06/28/92⁻–06/28/92⁺)
Δσf (bars)
A
μ'=0.7
Depth (km)
0
4
8
12
16
0
10
20
30
40
3
2.5
2
1.5
1
0.5
0
-0.5
-1
-1.5
-2
-2.5
-3
-3.5
Coseismic + Postseismic (06/28/92⁻–08/16/99⁻)
B
μ'=0.7
SE
NW
Along–strike distance (km)
Postseismic (06/28/92⁺–08/16/99⁻)
C
μ'=0.7
0.8
0.6
0.4
0.2
-0.2
-0.4
-0.6
-0.8
-1
Hector Mine coseismic slip distribution (meters)

Figure 6

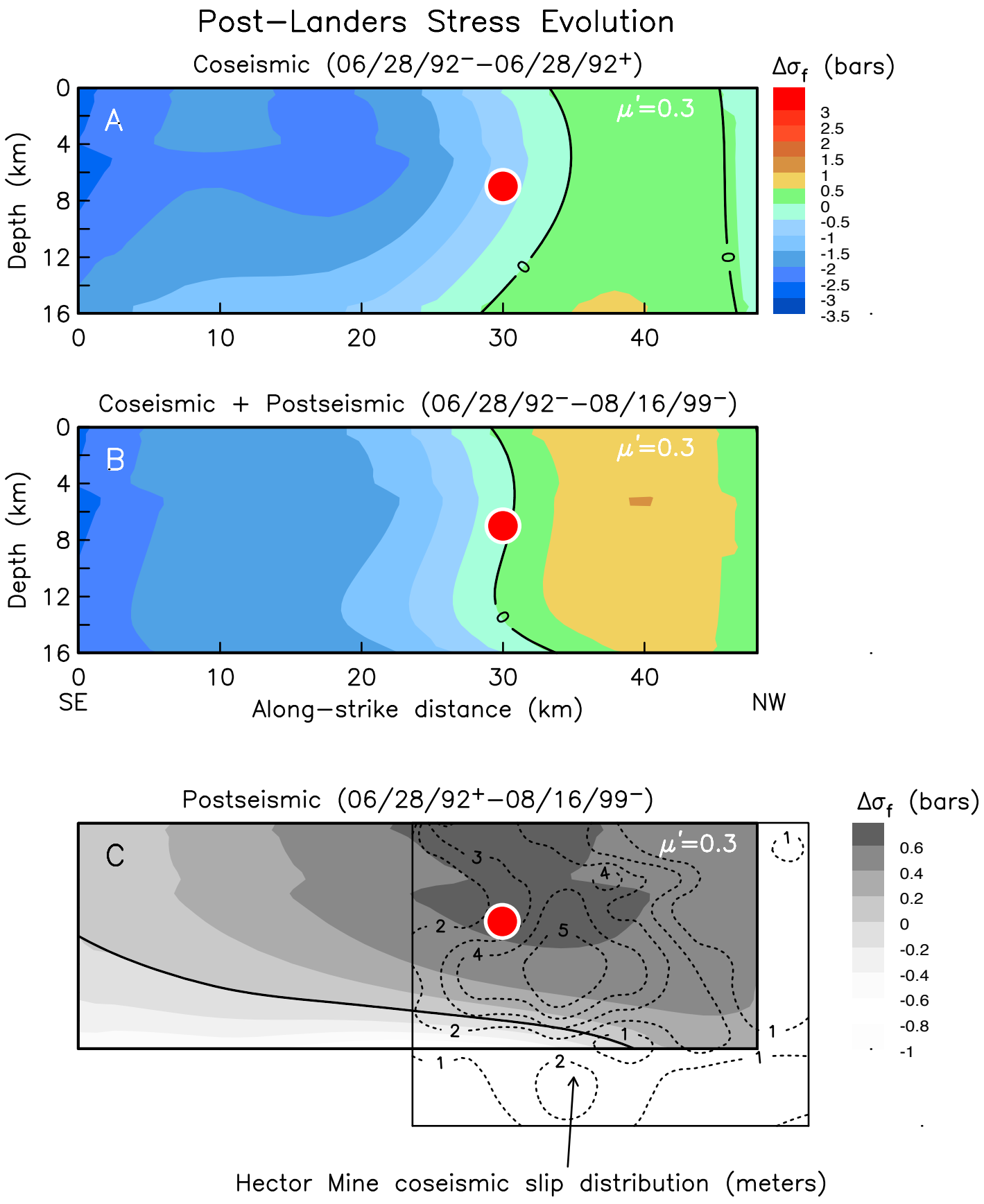
Post−Landers Stress Evolution
Coseismic (06/28/92⁻−06/28/92⁺)
Δσf (bars)
A
μ′=0.3
Depth (km)
Coseismic + Postseismic (06/28/92⁻−08/16/99⁻)
B
Along−strike distance (km)
SE
NW
Postseismic (06/28/92⁺−08/16/99⁻)
C
Hector Mine coseismic slip distribution (meters)